NJC

Accepted Manuscript

ROYAL SOCIETY OF CHEMISTRY

www.rsc.org/njc

Journal Name

ARTICLE

Room temperature synthesis of flower-like CaCO$_3$ architectures

Lu-feng Yang,[ab] De-qing Chu,*[ab] Hui-lou Sun,[a] and Ge Ge[a]

Shape-controlled crystallization of high-ordered three-dimensional (3D) hierachical flower-like vaterite calcium carbonate (CaCO$_3$) architecture was successfully prepared from a mild water-urea mixed system by a simple precipitation method. The mechanism of the crystal growth of CaCO$_3$ was expounded according the results, which is a step-by-step build process. It is found that the reaction time and the concentrations of carbonate and urea turned out to be important parameters for the control of morphology and polymorph of CaCO$_3$. The detailed morphology and polymorph of the synthesized hierarchical CaCO$_3$ nanostructures were characterized by Scanning electron microscopy (SEM), X-ray diffraction (XRD), Fourier transform infrared spectroscopy (FT-IR), Transmission electron microscope (TEM) and Electron diffraction (ED). This research may provide a promising route for the selective synthesis of other inorganic materials with different morphologies and polymorphs.

Introduction

The development of bottom-up crystallization strategies to fabricate single crystals patterned at the micro- and nanoscale remains an attractive challenge since these patterned structures are useful materials in various technological fields and important components in electronic, optical, sensory devices and so on.[1] One of the main goals of material science is to find new processing routes for the fabrication of advanced materials. A frequently used approach to achieve this is to mimic strategies applied by Nature to produce materials with hierarchical structure and superior properties. Inspired by exquisite control that biological systems exert over the nucleation and growth of biominerals, many efforts have been made to understand biomineralization principles and to develop bio-inspired strategies for the controlled synthesis of advanced inorganic materials.[2-4]

Understanding crystal growth is of great practical importance. The properties of a material greatly depend on its crystal structure and the size, morphology and texture of the crystals. It is thus important to understand the mechanism of growth so that a crystal can be tailored for a given application.[5] In the past years, research on biomimetic mineralization has demonstrated the existence of alternative crystallization pathways where, unlike the classical picture, crystal growth proceeds via (oriented) attachment of primary nanoparticle units,[6-8] potentially leading to complex ultrastructures of small building blocks.[9-11] For example, it was shown that synthetic organic polymers, capable of interacting with the as-formed particles, can induce self-organization of the building units on the mesoscale and prevent their fusion to a single crystal. This has principally been achieved by placing particular emphasis on CaCO$_3$ and silica systems and illustrating with other materials where it was considered appropriate. CaCO$_3$ provides an excellent example for illustrating morphogenesis strategies of single-crystal and polycrystalline materials. It is one of the most widely studied biominerals, because of both its high abundance and rich polymorphism, and it has been widely used as a model mineral in biomimetic experiments, leading to increased understanding of the mechanisms of biogenic control over mineral polymorph, orientation, and morphology. Providing a suitable example for illustrating morphogenesis strategies applicable to amorphous minerals.

CaCO$_3$ occurs in three anhydrous crystalline polymorphic forms, namely calcite, aragonite, and vaterite.[12, 13] Calcite is the most stable phase under ambient conditions, aragonite usually forms at elevated temperature, and vaterite is particularly the most unstable phases.[14] This, in turn, leads to the application of more stringent synthetic conditions, such as elevated temperature and pressure, and use of nonaqueous solvents and additives, to facilitate the selective precipitation of the desired metastable phase. Vaterite is the most unstable phase among three different types of crystalline polymorphs of CaCO$_3$ (aragonite, calcite, and vaterite) that are crystallized from amorphous calcium carbonate (ACC).[15] The inherent energetic instability of vaterite results in the phase transformation to other stable crystalline phases in aqueous solution, which occurs via a dissolution and recrystallization process (i.e., the dissolution of metastable phase and the growth of stable phase).[16] Stabilizing the vaterite phase has been one of major issues in biomineralization studies, not only because of its

[a.] College of Environment and Chemical Engineering, Tianjin Polytechnic University, Tianjin 300387, P.R. China.
   Fax: +86-22-83955762; Tel: +86-22-83955762; E-mail: dqingchu@163.com
[b.] State Key Laboratory of Hollow-Fiber Membrane Materials and Membrane Processes, Tianjin 300387, P.R. China.
   Fax: +86-22-83955762; Tel: +86-22-83955762;

rareness due to its intrinsic instability, but also because of its potential for biomedical and industrial applications since vaterite exhibits unique properties such as high surface area, solubility, dispersion, and a smaller specific gravity than calcite or aragonite.[17] Elucidating the vaterite growth mechanism and structure characteristics will expand our knowledge on how organisms control carbonate morphologies and polymorph selections and may improve the engineering applications of vaterite as an industrial material. Hence, the formation and stabilization mechanism of vaterite has aroused the interest of both scientists and engineers. Recently, Kabalah-Amitai et al.[18] found that the structure of vaterite is actually composed of at least two different crystallographic structures that coexist within a pseudo-single crystal. Demichelis et al.[19] also regarded vaterite as a group of related structures that differ in the order of stacking within the carbonate layers, rather than as a single disordered material. However, vaterite particles do not show well-defined morphologies, and usually aggregate into polycrystalline spheres.[20] In addition, different methods render different characteristics for vaterite crystallization. Such as growth kinetics and crystal stability, among which the morphology may be the most uncertain characteristic because it displays a great deal of variety. Currently, controlled morphology studies on vaterite $CaCO_3$ have received much attention in recent years. Sub-micron-sized vaterite tubes could be formed through nanobubble-templated crystal growth.[21] Vaterite nanowires were reported through the interaction of a polyelectrolyte with a self-assembled organic monolayer.[22] Nanorods of vaterite have been synthesized for the first time by the microemulsion method using CTAB as cationic surfactants.[23] Dagger-like vaterite particles have been prepared by a fast microwave-assisted method.[24] However, how these morphologies develop, what the texture of the resultant crystal is, and what the different shapes have in common, remains to be addressed.

In this study, we investigated the crystallization of $CaCO_3$ from a mild water-urea mixed system. The effects of experimental conditions including the reaction time and the concentrations of carbonate and urea on the crystal form and morphology of the as-prepared $CaCO_3$ were investigated. Specially, the 3D hierarchical flower-like vaterite $CaCO_3$ crystals can be selectively synthesized by adjusting experimental conditions. The crystallographic characteristics and growth process of the flower-like vaterite are investigated to shed light on the different stages of the crystallization mechanism of vaterite.

Experimental

Synthesis of the samples

All chemicals were of analytical grade used without further purification, and the water used in all experiments was doubly distilled water. In a typical synthesis procedure, 3D hierarchical flower-like vaterite $CaCO_3$ crystal aggregates were obtained from the reaction of $CaCl_2$, $NaHCO_3$ and Na_2CO_3 in a binary mixed system of water and urea. Firstly, aqueous

solution of Na_2CO_3 (2 M), $NaHCO_3$ (4 M) and $CaCl_2$ (1 M) were prepared as stock solution, and in a standard synthesis, two solutions of Na_2CO_3 (2 M, 1.25 mL) and $NaHCO_3$ (4 M, 1.25 mL) were sequentially injected into a 20 mL of 45wt% of urea solution. Then a solution of $CaCl_2$ (1 M, 2.5 mL) was injected into the above mixed solution under vigorously magnetic stirring by using a magnetic stirrer. In the total reaction volume of 25 mL, the final concentration of the Na_2CO_3, $NaHCO_3$ and $CaCl_2$ was 100 mM, 200 mM, and 100 mM, respectively. The obtained mixture was stirred for 120 min at room temperature (24 ℃ ± 1 ℃). Finally, the products were collected after centrifugation, washing with doubly distilled water and anhydrous ethanol, and drying at 60 ℃ under vacuum for 12 h and afterwards stored in a desiccator for further characterization.

Characterization

The XRD pattern of the products was recorded with a D8 X-ray diffractometer (Bruker, Germany) with graphite-monochromated Cu-Kα radiation (λ=1.542 Å), operating at 40 kV and 40 mA. SEM (Hitachi S-4800) was used to observe the resulting $CaCO_3$ precipitates with an accelerating voltage of 10 kV. TEM observation and electronic diffraction (ED) detection experiments were carried out with a JEM-2100F. FT-IR spectrometry was performed with a Bruker TENSOR 37 FT-IR analyzer.

Results and discussion

The formation of $CaCO_3$ flower-like nanostructures was investigated, which was based on the reaction of calcium ion and carbonate ion in the presence of urea molecule at room temperature. By adjusting the reaction time, concentrations of carbonate and urea, we obtained different morphologies and polymorph of $CaCO_3$ nanostructures. The detailed results and discussion were shown as follows.

Morphology and phase composition of the as-obtained $CaCO_3$ flower-like nanostructure

Fig. 1 presents scanning electron microscopy (SEM) and X-ray diffraction (XRD) images of the as-prepared 3D hierarchical flower-like vaterite $CaCO_3$. The flower-like $CaCO_3$ sample was obtained by the reaction of calcium ion and carbonate ion ([Na_2CO_3] = 2 M, [$NaHCO_3$] = 4 M, ω_{urea}= 45wt%, t = 120 min, 24 ℃ ± 1 ℃). A panoramic morphology of the product is displayed in Fig. 1(a), indicating the high yield and uniformity. A magnified SEM image showing the close observation of the nanostructures is given in Fig. 1(b). It reveals that the detailed morphology of $CaCO_3$ products is well-defined flower-like vaterite with diameters in the range of 3.6-4.2 μm. A close-up view of the flower-like nanostructures in Fig. 1(c) demonstrates the "petals" are about 200 nm in diameters and 1 μm in length, and they regularly contacted with each other into flower-like structures. It is worth noting that the flower "petals" grow out of opposite sides to show a decussate feature.

COMMUNICATION
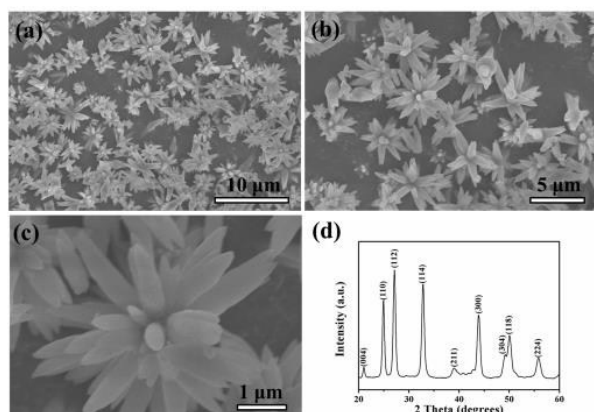
Fig. 1 SEM images and XRD pattern of 3D hierarchical flower-like vaterite $CaCO_3$ nanostructures {Prepared at (24 ℃ ±1 ℃), [Na_2CO_3] = 2 M, [$NaHCO_3$] = 4 M, ω_{urea}= 45wt%, t = 120 min}: (a) Overall product morphology; (b) Magnified SEM image; (c) Detailed view on an individual flower; (d) Representative XRD pattern recorded for perfect flower-like $CaCO_3$ synthesized in this work (V: vaterite).

The overall crystallinity and purity of the as-synthesized flower-like vaterite $CaCO_3$ were examined by X-ray diffraction (XRD) measurements. The XRD pattern of the as-synthesized flower-like $CaCO_3$ crystals confirms the structure of the vaterite (JCPDS 25-0127). The Bragg reflection peaks for the vaterite crystals obtained after 120 min at 2θ angles of 20.77, 24.70, 26.90, 32.60, 38.65, 43.65, 48.75, 49.70, 55.50 ° were corresponding to (004), (110), (112), (114), (211), (300), (304), (118) and (224) crystallographic planes, respectively (Fig. 1(d)), indicating that the composition of the $CaCO_3$ crystals was pure phase of vaterite. The particle size determined by the Debye–Scherrer formula is about 115 nm.
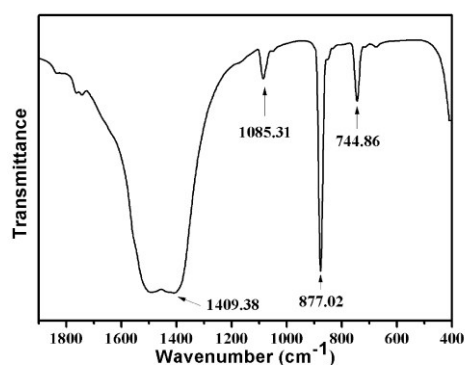
Fig. 2 FT-IR spectrum of the as-prepared perfect 3D flower-like hierarchical vaterite $CaCO_3$ nanocrystals {Prepared at (24 ℃ ± 1 ℃), [Na_2CO_3] = 2 M, [$NaHCO_3$] = 4 M, ω_{urea}= 45wt%, t = 120 min}.

The results were further demonstrated by FT-IR analysis as given in Fig. 2. In FT-IR spectrum, the absorption bands at 744.86, 877.02, 1085.31 and 1409.38 cm-1 showed the presence of the vaterite polymorph. No absorption bands at 854, 712, 700 cm^{-1} and 848, 714 cm^{-1} corresponding to aragonite and calcite, respectively, were recorded.[25] The SEM, XRD, and FT-IR observations indicate that metastable vaterite superstructures can be efficiently prepared during the mineralization of $CaCO_3$ with the appropriate concentrations of carbonate and urea, and reaction time.

Effects of reaction time

To reveal the forming process and growing mechanism of the flower-like vaterite $CaCO_3$ nanostructures, we have investigated the growth process systematically by analyzing the samples captured at different growth stages. A marked dependence of the crystal morphology on the structure evolution was observed for the product, and SEM and TEM images of the samples with different morphology are shown in Fig. 3. After conducting the reaction for 5 min, a typical $CaCO_3$ nanorod structure was obtained (Fig. 3(a)). Furthermore, it was found that the nanorod-structured $CaCO_3$ crystals are rather regular in shape. The length of a single nanorod is about 1–2 μm, and its maximum width was about 300 nm in the middle. In the terminal region, the width became close to 100 nm. The magnified image (Fig. 3(b)) shows that the detailed surface structures are rather coarse.
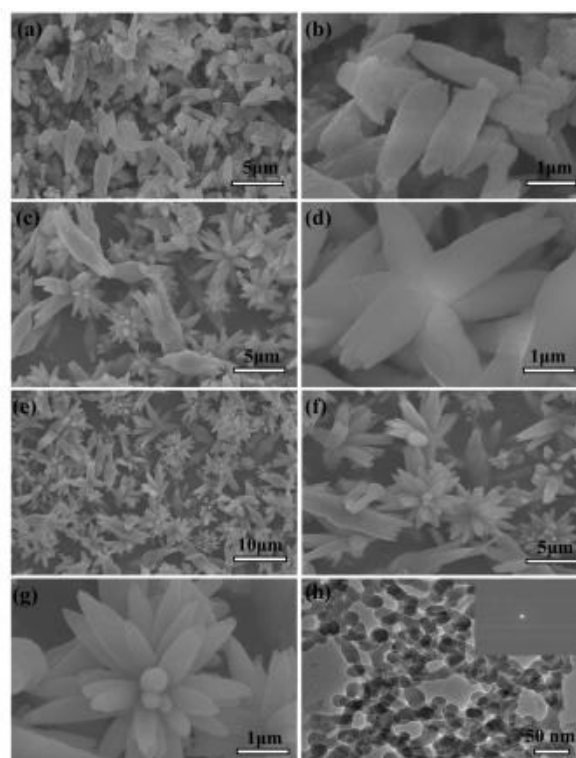
Fig. 3 SEM images of the $CaCO_3$ samples obtained after conducting the reaction for different time: (a and b) t=5 min; (c and d) t=30 min; (e, f and g) t=60 min; (h) TEM image of the early stage (about 1 min) of the $CaCO_3$ crystallization period. The inset in (h) indicates ED patterns of $CaCO_3$. {Prepared at (24 ℃ ± 1 ℃), [Na_2CO_3] = 2 M, [$NaHCO_3$] = 4 M, ω_{urea}= 45wt%}.

By further prolonging the reaction time to 30 min, the intermediate structures develop into initial 3D flower-like CaCO$_3$ nanostructures (Fig. 3(c)) via a surface reconstruction process. A close inspection of the flower-like structures is shown in Fig. 3(d). However, some nanorod-shaped crystals can also be discerned from Fig. 3(c). With the extension of the reaction time to 60 min, a mass of flower-structured grains can be clearly distinguished as shown in Fig. 3(e). The magnified image (Fig. 3(f)) shows the detailed flower-like structures. It is well known that the structures of products prepared by solution reactions depend on the rate of nucleation and growth of the reaction products. The results show that the rate of growth of CaCO$_3$ is faster than that of its nucleation. The growth rates of various surfaces can also be kinetically controlled, especially in the case of solution-phase synthesis at low temperatures. Due to the preferential growth of CaCO$_3$ in a certain direction, the flower-like products were obtained. The nanoparticle-mediated self-organization process of the mineralized products could be further inferred with the aid of magnified SEM images (Fig. 3(g)). The evolution of the crystal structure was determined by XRD measurement. The resulting samples were also mainly composed of vaterite crystals (Fig. 4), and the particle size determined from the XRD data with the Debye–Scherrer formula were about 35, 45, and 105 nm, respectively.
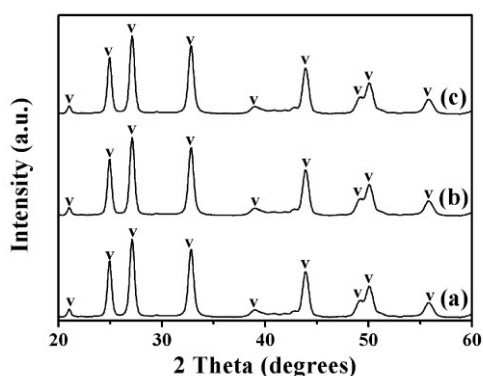
Fig. 4 XRD patterns of CaCO$_3$ crystals obtained after conducting the reaction for different time: (a) t = 5 min; (b) t = 30 min; (c) t = 60 min (V: vaterite). {Prepared at (24 °C ± 1 °C), [Na$_2$CO$_3$] = 2 M, [NaHCO$_3$] = 4 M, ω_{urea}= 45wt%}.

To obtain a better understanding of the self-assembly crystal growth mechanism, it is necessary to capture the initial intermediate before the petal-like vaterite crystal aggregates formed. Herein, TEM observation and electronic diffraction (ED) detection was employed to investigate the formation of the petal-like CaCO$_3$ crystals. This was achieved initially by using a small amount of CaCl$_2$, immediately dripping the mixture of Na$_2$CO$_3$, NaHCO$_3$ and urea solution onto a copper grid (the copper grid was placed on a filter paper), and naturally drying (about 1 min). At the onset, the image of the original sample, shown in Fig. 3(h), indicated that nearly spherical nanoparticles (around 25 nm in size) with a rough profile and no clear boundaries formed. A clear dispersion ring from the

ED indicated that CaCO$_3$ was in the amorphous phase (inset of Fig. 3(h)).

Effects of concentration of carbonate

In our synthesis, we found that by controlling experimental parameters such as the concentrations of carbonate and urea, various structures and morphology of CaCO$_3$ can be obtained. The different morphologies of the CaCO$_3$ nanostructures shown in Fig. 5 are created by varying only the concentration of NaHCO$_3$. When the added NaHCO$_3$ was decreased from 4 M to 2 M (pH = 10.95) or 1 M (pH = 11.24), the resulting samples were also mainly composed of flower-like crystals, as shown in Fig. 5((c) and (d)) and Fig. 5((e) and (f)); nevertheless, the flower structures of the CaCO$_3$ particles changed to be extremely defective. Furthermore, in the absence of NaHCO$_3$ (pH = 12.17), the resulting CaCO$_3$ particles were completely wintersweet-structured crystals as shown in Fig. 5((a) and (b)).
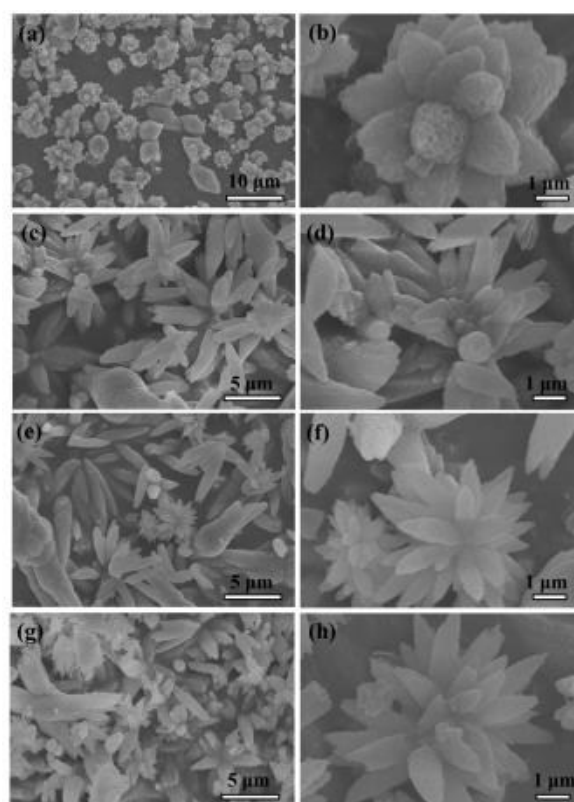
Fig. 5 SEM images of the CaCO$_3$ samples produced with different concentrations of NaHCO$_3$: (a and b) 0 M; (c and d) 1 M; (e and f) 2 M; (g and h) 8 M. {Prepared at (24 °C ± 1 °C), [Na$_2$CO$_3$] = 2 M, ω_{urea}= 45wt%, t = 120 min}.

XRD spectra in Fig. 6(a)–(c) show that peak intensities for vaterite (JCPDS 33-0268) increase, whereas those for calcite (JCPDS 47-1743) increase firstly and then decrease with increasing NaHCO$_3$ concentration.
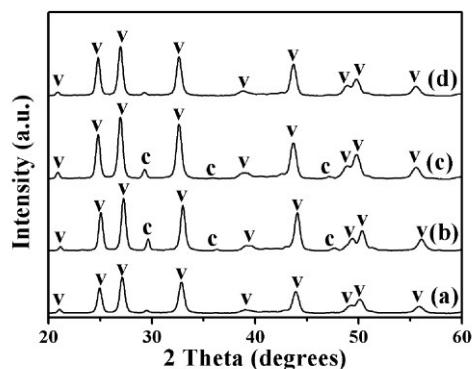
Fig. 6 XRD patterns of $CaCO_3$ crystals produced with different concentrations of $NaHCO_3$: (a) 0 M; (b) 1 M; (c) 2 M; (d) 8 M (C: calcite, V: vaterite). {Prepared at (24 ℃ ±1 ℃), $[Na_2CO_3]$ = 2 M, ω_{urea}= 45wt%, t = 120 min}.

In addition, if the amount of $NaHCO_3$ was increased to 8 M (pH = 10.24), then the composition of the $CaCO_3$ particles displayed relatively pure vaterite dandelion-like structures (Fig. 5((g) and (h)) and 6(d)). By increasing the amount of $NaHCO_3$, the total carbonate content of the system (and thus the pH value) is essentially changed. Under a given set of conditions this will lead to higher supersaturation, which favors faster precipitation of the kinetic phase, that is, the vaterite phase from the viewpoint of kinetics as reported by Ogino et al.[26] and Xyla et al.,[27] and thus changes in precipitation kinetics. The results demonstrate that phase switching can be achieved by changing the kinetic control. Ostwald's Rule of Stages can offer an explanation for this observation.

Effect of concentration of urea

It is also worth mentioning that the concentration of urea in this system is important in determining the morphologies and polymorph of the $CaCO_3$ crystals. The different morphologies of the $CaCO_3$ nanostructures shown in Fig. 7 are created by varying only the concentration of urea. When the added urea was decreased from 60wt% (pH = 10.86) to 45wt%, 30wt% (pH = 10.53) or 15wt% (pH = 10.40), the resulting samples were also mainly composed of flower-like crystals, as shown in Fig. 7((c and d), (e and f), and (g and h)); nevertheless, the flower structures of the $CaCO_3$ particles changed to be extremely defective. Furthermore, in the absence of urea (pH = 10.26), the resulting $CaCO_3$ particles were completely nanorod-structured crystals as shown in Fig. 7((a) and (b)). XRD spectra in Fig. 8(a)–(d) show that peak intensities for vaterite (JCPDS 33-0268) decrease, whereas those for calcite (JCPDS 47-1743) increase with increasing urea concentration. By increasing the amount of urea, the total carbonate content of the system (and thus the pH value) is essentially changed. This observation suggested that the presence of urea had an obvious influence on the morphology and phase structure of $CaCO_3$ particles, probably due to a strong interaction between the carbanyl group of urea and the Ca^{2+} ions, which influenced the nucleation and growth of $CaCO_3$ particles.
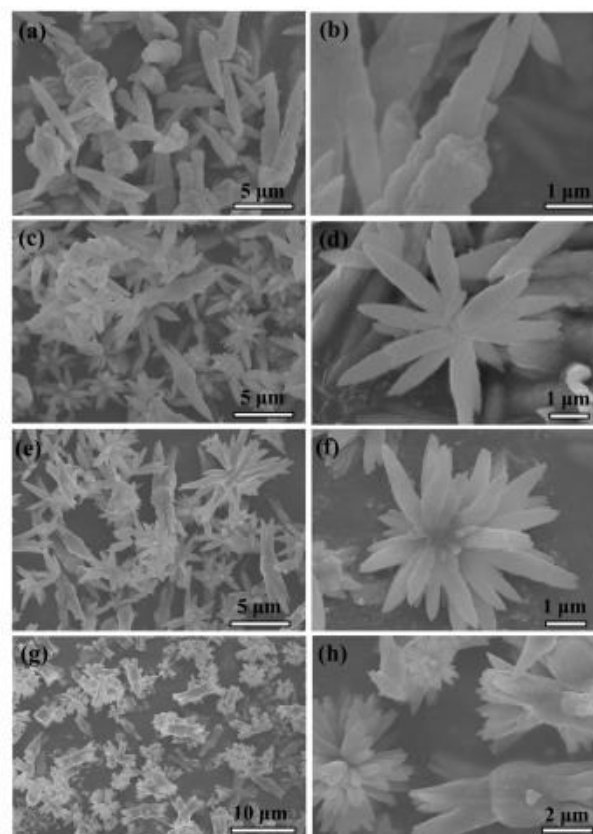
Fig. 7 SEM images of the $CaCO_3$ samples produced with different concentrations of urea: (a and b) 0wt%; (c and d) 15wt%; (e and f) 30wt%; (g and h) 60wt%. {Prepared at (24 ℃ ±1 ℃), $[Na_2CO_3]$ = 2 M, $[NaHCO_3]$ = 4 M, t = 120 min}.

Higher concentration of urea in the mixed system would inhibit the formation of vaterite phase, meanwhile promoting the formation of thermodynamically stable calcite phase. The increasing urea concentration results in the increase of both bulk and packing densities.[28] According to the nucleation and growth theory,[29] to form a new nucleator, an activation energy (ΔG_N) must be overcome. ΔG_N can be expressed as: $\Delta G_N =16\pi(\Delta G_1)^3/3(kT \ln S)^2$, where ΔG_1 is the surface energy that is needed to form the new interface and maintain the crystal growth, k the Boltzmann constant, T the temperature, and S the supersaturation of solution. Thus, the decrease of the surface energy ΔG_1 or the increase of the supersaturation S can reduce the activation energy for the nucleation of $CaCO_3$. In the presence of urea, the nucleation of $CaCO_3$ often occurs in the chemical microenvironments near the region of urea chains. In these microenvironments, there is an organic–inorganic interface region, and more Ca^{2+} and CO_3^{2-} ions were enriched. Therefore, the supersaturation of $CaCO_3$ in this interface region is higher than that in the bulk solution, which results in facile nucleation of $CaCO_3$ due to a decrease of the activation energy. A large number of small $CaCO_3$ primary particles are formed at an outburst speed and these nuclei are adsorbed on the chains of polymers by covalent action between Ca^{2+} ions on the surface of $CaCO_3$ and carbanyl groups on the chains of urea. During the growth of $CaCO_3$, the urea further adsorbs on the surface of the as-formed $CaCO_3$ and prevents the further growth of particles along specific planes, which leads to

flower-like morphology. This inhibiting action increases with the increasement of the concentration of urea.
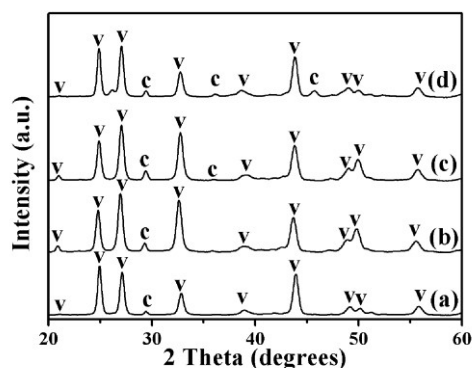
Fig. 8 XRD patterns of $CaCO_3$ crystals produced with different concentrations of urea: (a) 0wt%; (b) 15wt%; (c) 30wt%; (d) 60wt% (C: calcite, V: vaterite). {Prepared at (24 ℃ ± 1 ℃), $[Na_2CO_3]$ = 2 M, $[NaHCO_3]$ = 4 M, t = 120 min}.

Formation mechanism of the as-obtained 3D hierarchical flower-like $CaCO_3$ nanostructures

Our results show that flower-like crystals can be synthesized by adjusting the reaction time, concentration of carbonate and urea. Based on the above observations, a mechanism of formation of the flower-like crystals is proposed as follows. It could be assumed that the formation of the flower-like structure was controlled not only by the growth thermodynamics, but also by the growth kinetics. The formation process could be purposely divided into several processes: (i) formation of the primary nanocrystals, (ii) growth of the secondary structure and (iii) formation of the three-order structure. The growth mechanism is similar to those of the branched ZnO[30] and Cu_2O crystals.[31] Fig. 9 was used to illustrate the formation of the as-obtained $CaCO_3$ flower-like nanostructures. In the first stage, the crystal nucleated from the precursor solution. Then the nanoparticles were formed and fused with each other to reduce the overall energy. These nanocrystals grew into the pristine nanorods ($CaCO_3$ petals) through the dissolution/crystallization process, and the small petals further grew into the large ones. At the same time, the nanocrystals grew on these petals sequentially. After that, the self-assembly of petals resulted in the formation of initial $CaCO_3$ flower-like nanostructures. The petals may fuse "head-to-head" to form the flower-like nanostructures. As the crystal growth proceeded, the fully bloomed $CaCO_3$ flowers were obtained. However, the real mechanism involved in the system is rather complicated and needs more dedicated work in the future.
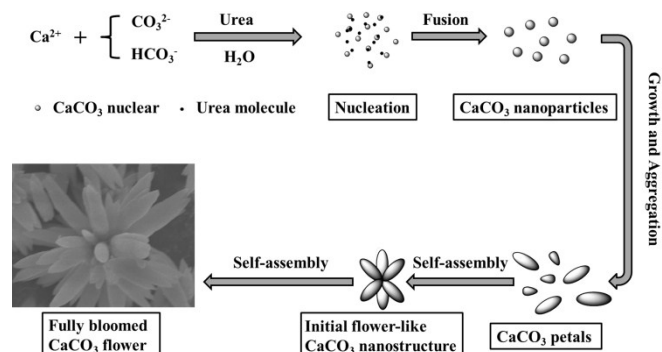
Fig. 9 Schematic illustration of the formation of the 3D hierarchical $CaCO_3$ flower-like nanostructures.

Conclusions

In summary, unique 3D hierarchical flower-like vaterite $CaCO_3$ crystal aggregates was successfully synthesized in the water-urea mixed system, for the first time. The precipitated $CaCO_3$ polymorph, and its morphology, can be controlled by selecting specific formation conditions from an experimental matrix of reaction time, and concentrations of carbonate and urea. The reaction time, and the concentrations of carbonate and urea turned out to be important parameters for the control of morphologies and polymorph of $CaCO_3$. Moderate concentrations of carbonate and urea facilitate the formation of flower-like vaerite. Unique 3D flower-like $CaCO_3$ crystals were obtained at adequate reaction time. It is believed that such polycomponent systems may offer a new way to control the morphology and polymorph of more complex crystalline 3D structures of $CaCO_3$ and other inorganic materials and could be extended to other systems.

Acknowledgements

Notes and references

1.   J. Aizenberg, D. A. Muller, J. L. Grazul and D. Hamann, *Science*, 2003, **299**, 1205-1208.
2.   S. Mann, *Nature*, 1993, **365**, 499-505.
3.   E. Dujardin and S. Mann, *Advanced Materials*, 2002, **14**, 775.
4.   H. Colfen and S. Mann, *Angew Chem Int Ed Engl*, 2003, **42**, 2350-2365.
5.   C. Burda, X. Chen, R. Narayanan and M. A. El-Sayed, *Chemical reviews*, 2005, **105**, 1025-1102.
6.   D. Li, M. H. Nielsen, J. R. Lee, C. Frandsen, J. F. Banfield and J. J. De Yoreo, *Science*, 2012, **336**, 1014-1018.
7.   R. L. Penn and J. F. Banfield, *Science*, 1998, **281**, 969-971.
8.   A. Van Driessche, L. Benning, J. Rodriguez-Blanco, M. Ossorio, P. Bots and J. García-Ruiz, *Science*, 2012, **336**, 69-72.
9.   H. Colfen and M. Antonietti, *Angew Chem Int Ed Engl*, 2005, **44**, 5576-5591.

10. M. Niederberger and H. Colfen, *Physical chemistry chemical physics : PCCP*, 2006, **8**, 3271-3287.
11. S. Mann, *Nature materials*, 2009, **8**, 781-792.
12. A. Sarkar and S. Mahapatra, *Crystal Growth & Design*, 2010, **10**, 2129-2135.
13. H. Cölfen, *Current Opinion in Colloid & Interface Science*, 2003, **8**, 23-31.
14. S. I. Kuriyavar, R. Vetrivel, S. G. Hegde, A. V. Ramaswamy, D. Chakrabarty and S. Mahapatra, *Journal of Materials Chemistry*, 2000, **10**, 1835-1840.
15. E. M. Pouget, P. H. Bomans, J. A. Goos, P. M. Frederik and N. A. Sommerdijk, *Science*, 2009, **323**, 1455-1458.
16. N. Spanos and P. G. Koutsoukos, *Journal of Crystal Growth*, 1998, **191**, 783-790.
17. K. Naka, Y. Tanaka and Y. Chujo, *Langmuir*, 2002, **18**, 3655-3658.
18. L. Kabalah-Amitai, B. Mayzel, Y. Kauffmann, A. N. Fitch, L. Bloch, P. U. Gilbert and B. Pokroy, *Science*, 2013, **340**, 454-457.
19. R. Demichelis, P. Raiteri, J. D. Gale and R. Dovesi, *Crystal Growth & Design*, 2013, **13**, 2247-2251.
20. K. K. Sand, J. D. Rodriguez-Blanco, E. Makovicky, L. G. Benning and S. L. S. Stipp, *Crystal Growth & Design*, 2012, **12**, 842-853.
21. Y. Fan and R. Wang, *Advanced Materials*, 2005, **17**, 2384-2388.
22. M. Balz, H. A. Therese, J. Li, J. S. Gutmann, M. Kappl, L. Nasdala, W. Hofmeister, H. J. Butt and W. Tremel, *Advanced Functional Materials*, 2005, **15**, 683-688.
23. J. Ahmed, Menaka and A. K. Ganguli, *CrystEngComm*, 2009, **11**, 927.
24. R.-J. Qi and Y.-J. Zhu, *The Journal of Physical Chemistry B*, 2006, **110**, 8302-8306.
25. J. Chen and L. Xiang, *Powder Technology*, 2009, **189**, 64-69.
26. T. Ogino, T. Suzuki and K. Sawada, *Geochimica et Cosmochimica Acta*, 1987, **51**, 2757-2767.
27. A. G. Xyla, E. K. Giannimaras and P. G. Koutsoukos, *Colloids and Surfaces*, 1991, **53**, 241-255.
28. K. Białowicz and U. Kiełkowska, *Polish Journal of Chemical Technology*, 2014, **16**, 95-98.
29. J. Ouyang, *Science in China Series B*, 2003, **46**, 234.
30. B. Liu and H. C. Zeng, *Journal of the American Chemical Society*, 2003, **125**, 4430-4431.
31. H. Zhang, X. Zhang, H. Li, Z. Qu, S. Fan and M. Ji, *Crystal growth & design*, 2007, **7**, 820-824.
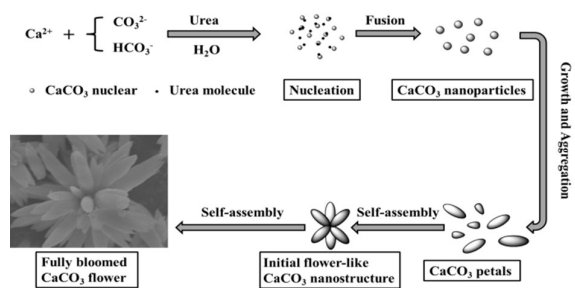
Proposed hierarchical self-assembly mechanism of the formation of flower-like vaterite superstructures.